Radiolabeling of Biodegradable Polymeric Microspheres with $[^{99m}Tc(CO)_3]^+$ and *in Vivo* Biodistribution Evaluation using MicroSPECT/CT Imaging

Katayoun Saatchi and Urs O. Häfeli*

Faculty of Pharmaceutical Sciences, University of British Columbia, 2146 East Mall, Vancouver, BC V6T 1Z3, Canada.
Received February 11, 2009; Revised Manuscript Received April 22, 2009

Poly(L-lactide) (PLA) microspheres tailored with a tridentate chelating group were radiolabeled with $[^{99m}Tc(H_2O)_3(CO)_3]^+$ and optimized for labeling efficiency and stability. Various ligand−polymer blend compositions with commercial PLA (from 2% to 100%) were evaluated. Labeling efficiencies over 95% were achieved in a 5 min reaction using 100% of the ligand−polymer or within 15 min using a 5% ligand−polymer blend. The addition of 1.5% of PEGylated copolymer to the blend did not affect the labeling efficiency of these particles but changed their *in vivo* behavior. MicroSPECT/CT imaging showed significant uptake of non-PEGylated microspheres by the murine lung, while only the liver and spleen took up PEGylated microspheres. Such ^{99m}Tc radiolabeled biodegradable microspheres will be useful diagnostic imaging agents for visualization of the functioning reticuloendothelial system (RES). Similarly, other sizes of the same microspheres will allow imaging of lung perfusion, bone marrow, lymph and inflammation scintigraphy, and radioembolization therapy.

INTRODUCTION

In nuclear medicine, particles of various sizes are radiolabeled to diagnose different conditions (*1*). The particle-bound radioactivity is made visible by imaging, typically with a single photon emission computed tomography (SPECT) instrument. Examples of such particle-based imaging include lung perfusion imaging with ^{99m}Tc-labeled macroaggregated albumin (MAA) particles sized between 10−90 μm (*2, 3*) liver and spleen function imaging with ^{99m}Tc-sulfur colloid sized 0.1−1 μm (*4, 5*) or with ^{99m}Tc-albumin colloid sized 0.4−2 μm (*6, 7*), both of which are taken up by the reticulo-endothelial system (RES); and bone marrow, inflammation, and lymph scintigraphy which uses even smaller, less than 0.08 μm, ^{99m}Tc-albumin colloid (*8, 9*).

A major drawback of these imaging methods is that the main material used to prepare the diagnostic radiopharmaceuticals is albumin, a human protein with all the inherent risks (e.g., hepatitis C, HIV) associated with blood products. To eliminate these risks and their associated liability, several manufacturers have taken albumin-based products (e.g., Technescan, Microlite, and Isojex) off the market.

Particulate radiopharmaceuticals used in nuclear medicine, including the nonalbumin ones (Table 1), are associated with a second disadvantage. Specifically, their wide size distribution results in an uptake by other than the target tissue or organ. As a result, higher background activities are seen in these areas, leading to the deterioration of the imaging signal and resulting in the need for higher injection activities in order to obtain statistically sound images from the imaging region. The high background makes it thus impossible to minimize the injected activity and, therefore, the radiation dose received by the patient.

To circumvent the problems associated with particulate albumin radiopharmaceuticals, we sought to develop a replacement particle of narrowly controlled size. Such particles would form the basis of a radiolabeling kit for the preparation of radioactive microspheres for both diagnostic and therapeutic applications. A successful radiolabeling kit must, in addition to containing nontoxic biodegradable microparticles of narrow size distribution, show excellent labeling efficiency and stability. Diagnostic applications of such radiopharmaceuticals in nuclear medicine include lung perfusion imaging, imaging of the reticuloendothelial system (RES) and of bone marrow, as well as inflammation and deep vein thrombosis imaging (Table 1). Therapeutic applications of such radiopharmaceuticals in radiation oncology include the radioembolization of liver tumors, uterine fibroids, meningiomas and arteriovenous malformations, and the local treatment of leftover and recurring disease (Table 1).

We have previously developed biodegradable microspheres (made of FDA-approved polylactide or polylactide-*co*-glycolide) that can be made in different sizes (*10, 11*) with relatively narrow size distributions. We have also synthesized tailored polymers to accommodate metal coordination using a simple one-pot synthesis of biodegradable tailored polylactide with a built-in tridentate ligand to coordinate selected metal ions, "polymers with a grip" (*12*) (Figure 1). To follow up on both of these studies, and to investigate a potential replacement product for the discontinued albumin-based particles (e.g., Microlite, Table 1), this work describes the radiolabeling of these custom polymers or a blend thereof with commercially available polymers in the shape of microspheres (0.5−1.5 μm) with $[^{99m}Tc(CO)_3]^+$ (Figure 1). The labeling conditions were also investigated and optimized for microspheres containing additional poly(ethylene glycol) (PEG) groups and then compared for their biological distribution in mice.

EXPERIMENTAL PROCEDURES

Materials. Poly(L-lactide) (PLA) with a molecular weight (MW) of 2 kDa was purchased from Boehringer Ingelheim (Resomer L104; Ingelheim, Germany). Poly(vinyl alcohol) (PVA) with a MW of 13−23 kDa and 98% hydrolyzed was obtained from Aldrich. All other chemicals were purchased from Sigma/Aldrich and used as received. The PEGylated copolymer $MePEG_{17}$-b-PCL_{10} was kindly provided by the Burt lab in the Faculty of Pharmaceutical Sciences at The University of British Columbia (*13*). Double-distilled water was used in all experiments.

* Corresponding author. Urs Hafeli, Faculty of Pharmaceutical Sciences, University of British Columbia, 2146 East Mall, Vancouver, BC V6T 1Z3, Canada; e-mail: uhafeli@interchange.ubc.ca; Tel. (604) 822-7133; Fax (604) 822-3035.

10.1021/bc900066j CCC: $40.75
Published on Web 06/03/2009

Table 1. Particle-Based Radiopharmaceuticals for Imaging and Therapy

radiopharmaceutical	particle size	application	labeling	availability	ref
^{99m}Tc-MAA	10−90 μm (90%), all <150 μm	lung perfusion imaging, detection of deep vein thrombosis in lower extremities	10 min @ RT[a]; >90%	Draximage, Pharmalucence	2, 3
^{99m}Tc-albumin colloid	0.4−2 μm	RES (liver, spleen) imaging	2 min @ RT; ∼100%	Microlite, Du Pont discontinued	6, 7
^{99m}Tc-albumin colloid	<0.08 μm, mean 0.03 μm	bone marrow imaging (15% of colloid ends up there), inflammation scintigraphy, lymphoscintigraphy	5−10 min@ RT; ∼100%	Nanocoll, Du Pont discontinued	8, 9
^{99m}Tc-sulfur colloid	0.1−1 μm (mean 0.3 μm)	liver and spleen imaging, bone marrow (2−5% ends up there) and lymph imaging, GI blood loss studies, gastric emptying studies (egg sandwich)	5−10 min @ boiling; >99%	Pharmalucence	4, 5
^{99m}Tc-antimony sulfur colloid	mean 0.01 μm	lymphoscintigraphy	30 min @ boiling; ∼100%	-	5, 30
^{32}P-chromic phosphate colloid	2 μm	treatment of peritoneal or pleural effusions caused by metastatic disease, interstitial injection	ready for injection	Phosphocol P32, Covidien	31−33
^{90}Y glass microspheres*	25−35 μm	radioembolization of liver tumors	neutron activation; 100%	Therasphere, MDS Nordion	34
^{90}Y resin microspheres*	25−35 μm	radioembolization of liver tumors	neutron activation; 100%	SIR-Spheres, SIRTEX	35

[a] RT = room temperature.

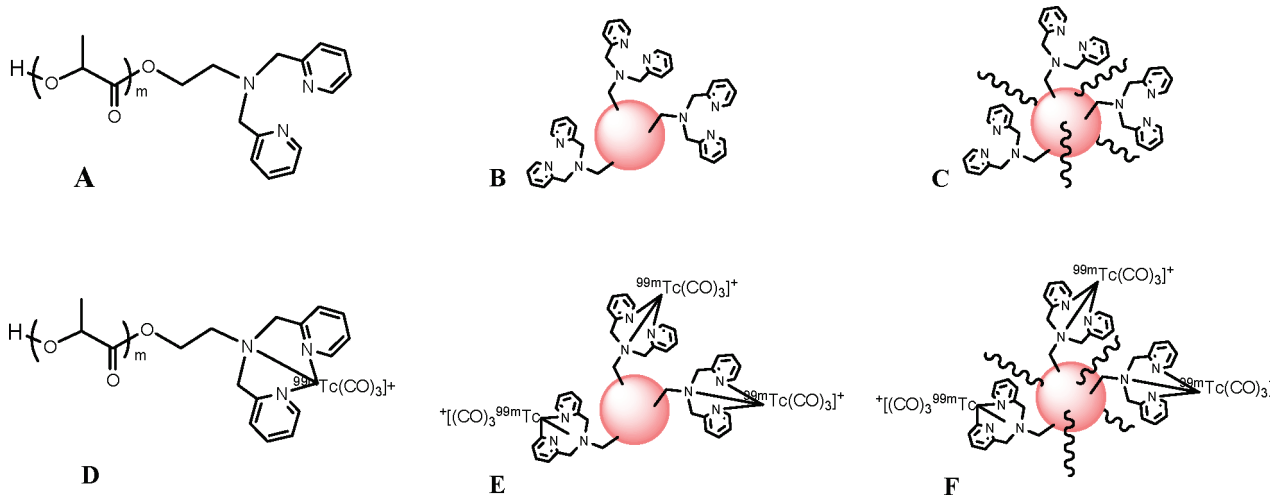

Figure 1. (A) Structure of "chelomer"; (B) cartoon of a microsphere with ligands on the surface; (C) PEGylated blend chelomer (wiggly line, PEG); D,E,F) Matching coordinated/radiolabeled chelomer and microspheres.

The radioisotope used herein,^{99m}Tc, is present in almost all particle-based radiopharmaceuticals including Technescan and Microlite and is currently the most used imaging agent in nuclear medicine due to its ideal physical properties ($t_{1/2}$ = 6 h, E = 140 keV, 89% abundance), suitable dosimetry (low radiation dose) and high specific activity. It is generator produced (^{99}Mo/^{99m}Tc) and available at a reasonable cost. The most recent labeling precursor to yield ^{99m}Tc radiopharmaceuticals is the $[^{99m}Tc(CO)_3(H_2O)_3]^+$ complex cation (*14, 15*). This complex is suitable for coordination to a wide variety of ligands, because it has a robust $[fac\text{-}Tc(CO)_3]^+$ core, a small size, and is kinetically inert and thermodynamically stable. Its three potential binding sites are readily available for coordination, since the aqua ligands are labile and easily replaced (*16*−*18*). We prepared the $[^{99m}Tc(H_2O)_3(CO)_3]^+$ precursor from Isolink kits generously provided by Mallinckrodt (now Covidien, St. Louis, MO).

Thin layer chromatography (TLC) was performed on black TEC-Control strips (Cat# 150−005; Biodex, Shirley, NY, USA) using saline as the mobile phase. The radioactive TLCs were made visible using a phosphor imager (Cyclone storage phosphor imager with 20 × 25 cm^2 phosphor screen, Perkin-Elmer, Waltham, MA, USA) and analyzed using OptiQuest software. Microspheres were separated by centrifugation using an Eppendorf Centrifuge 5415 C at 6000 rpm (6611 g). A polytron (PT 10/35; Kinematica, Lucerne, Switzerland) was used for homogenization during microsphere preparation. Scanning electron microscopy (SEM) was performed on a Hitachi S-3000N (acceleration voltage 20.0 KV, SE mode, 15.0 mm working distance). The particles were sputtered with a 10 nm layer of Au/Pd (60:40) prior to imaging. Activity measurements were carried out using a Packard Cobra II gamma counter (Perkin-Elmer).

Chelomer Preparation. The ligand-polymer, nick-named "*Chelomer*" in our laboratories (***Chel***ating Poly***mer***) (Figure 1A), was prepared by ring-opening polymerization of L-lactide as previously reported (*12*). Briefly, L-lactide was polymerized

using bis(2-(aminomethyl)pyridine)ethanol for the initiator and tin(octoate) as the catalyst at 125 °C for 3.5 h. The product was completely characterized before use by ^{1}H NMR, ^{13}C NMR, MALDI-TOF MS, and FTIR (*12*).

Microsphere Preparation. All microspheres were made using a double emulsion solvent evaporation technique (*19*). Briefly, the polymer(s) were dissolved in 4 mL of CH_2Cl_2. The first emulsion (w/o) was prepared by homogenization (27 000 rpm) of 400 μL H_2O in the polymer CH_2Cl_2 solution for 2.5 min in an ice bath. PVA (1% w/v, 15 mL) was added to this mixture and homogenized for another 2.5 min to make the second emulsion (w/o/w). This mixture was quickly poured into a stirred 1% solution of PVA (85 mL) at 2000 rpm for 5 min. Stirring continued for 2.5 h, after which the mixing speed was reduced to 500 rpm, and the suspension was stirred long enough for the foam to settle. The microspheres were washed several times in water by serial centrifugation at 5000 rpm (2683 g) and then resuspended in 1 mL water and stored at 4 °C. Since the microsphere preparation is just a physical transformation, no characterization was carried out to determine the nature of particles. However, the size and shape of the particles were measured using scanning electron microscopy.

Functionalized Microspheres. The chelomer and various blends (wt % mixture of the chelomer with commercial PLA) of chelomer with PLA were used to produce chelating microspheres. The 2% chelomer microspheres were, for example, made by dissolving 4 mg chelomer and 196 mg of PLA in 4 mL CH_2Cl_2. Additional microspheres containing 5%, 10%, 25%, and 100% chelomer were also produced, while 0% chelomer (= 100% PLA) microspheres were used as controls in all studies. Pegylated microspheres were made by blending (a) 5% chelomer, 1.5% $MePEG_{17}$-*b*-PCL_{10} with 93.5% PLA; and (b) 10% chelomer, 3% $MePEG_{17}$-*b*-PCL_{10} with 87% PLA.

Radiolabeling. The precursor complex $[^{99m}Tc(H_2O)_3(CO)_3]^+$ was prepared by injecting a saline solution of $Na[^{99m}TcO_4]$ (740−1850 MBq), diluted to 1 mL total volume with water, into the Isolink vial and heating for 25 min in boiling water. After cooling, the vial was vented and 0.2 mL HCl (0.1 M) added to neutralize the solution (pH = 7). The volume was adjusted to 2 mL with water. A >94% yield for the reaction was confirmed by TLC of the reaction mixture in saline, in agreement with the information provided by Covidien.

After addition of the desired activity A_T (9−260 MBq) to a 2 mg suspension of microspheres (total combined volume $V_T \leq 300$ μL), the mixture was heated to 75 °C, shaken at 1000 rpm for varying times (2 min to 2 h), and cooled to room temperature. At each time point, the suspension was centrifuged for 15 min at 6611 *g* and a known volume V_S (50 μL) of supernatant removed and its activity A_S measured. The labeling efficiency was then calculated with time-corrected activities as

$$\text{labeling efficiency}(\%) = \frac{A_S \times V_T}{V_S \times A_T} \times 100 \qquad (1)$$

Each experiment was performed with a minimum of 3 and up to 6 replicates. Microspheres made from commercial PLA were used as controls in all studies. Variables affecting labeling (heating time, heating temperature, chelomer fraction) were optimized to achieve maximum labeling efficiency at minimum heating time.

Cysteine Challenge. After radiolabeling, a 1 mM cysteine solution in PBS was added to the labeled microspheres to a total of 1 mL. The samples were shaken at 1000 rpm and 37 °C for 1 h, centrifuged, and the activity in 300 μL supernatant aliquots measured. Dissociation of $[^{99m}Tc(CO)_3]^+$ was measured by TLC. The remaining cysteine solution (700 μL) was shaken for an additional 23 h and another 300 μL supernatant aliquot analyzed. After the 48 h time point, the last aliquot was sampled, the radioactivity of all aliquots analyzed in a gamma counter, and the percentage of microsphere-bound activity calculated.

Biodistribution. To investigate if the microspheres were appropriate for RES imaging, the biodistribution of the 5% blended microspheres, with and without 1.5% of the PEGylated block copolymer, was determined using microSPECT/CT imaging on an X-SPECT instrument (Gamma Medica, Northridge, CA; now Siemens) at McMaster University's Centre for Preclinical and Translational Imaging in Hamilton, Ontario. Microspheres were labeled as explained above immediately prior to the imaging studies at the Nuclear Medicine Department's Radiopharmacy. Groups of four female PyVMT transgenic mice with mammary tumors and four female C57BL/6 mice with subcutaneous neck tumors grown from a primary cell line at passage six of PyVMT mouse tumors were injected intravenously into the tail vein with 18.5 MBq of the non-PEGylated microspheres and with 18.5 MBq of the ^{99m}Tc-tricarbonyl precursor, respectively. These mice were predestined to be sacrificed, so rather than healthy mice, they were used to give us the additional benefit of investigating tumor uptake for the precursor ^{99m}Tc-tricarbonyl complex and confirming no particle uptake in the tumor. Later, an additional group of four female C57BL/six mice without tumors received 18.5 MBq of the ^{99m}Tc-labeled PEGylated microspheres. At 2, 4, and 6 h after injection, a SPECT scan (32 projections for initially 18 s and at the later two time points 46 s) was performed under isoflurane anesthesia in the supine position, followed by a CT scan (512 projections), after which the animals were sacrificed and the organs removed, weighed, and their activity determined using a Packard Cobra II auto gamma-counter. Results were expressed as the percentage of the injected dose per organ and per gram of tissue (%ID/g), and the tumor-to-blood ratios calculated from the %ID/g values. The biodistribution of the precursor complex $[^{99m}Tc(H_2O)_3(CO)_3]^+$ was investigated and compared to that of the microspheres as a control.

RESULTS AND DISCUSSION

Biodegradable polymers for the delivery of radiation have been seriously under-investigated in nuclear medicine. Such polymers if designed properly are suitable tools for many different diagnostic or therapeutic applications. Depending on the polymer's physical shape, for example, in the form of microspheres and nanospheres, and the radioisotope used, these compounds can replace currently used products such as macroaggregated albumin particles, nonbiodegradable sulfur colloids, or even TheraSphere and SIR-Spheres (Table 1). In a different physical shape, for example, in the form of films, disks, and wafers, such a radiolabeled polymer could be used to deliver local radiation, in a similar way as the Gliadel wafers deliver an anticancer drug for the prevention of recurring disease.

Our goal in this work was to create a simple microsphere radiolabeling kit suitable for various *in vivo* applications. For this purpose, we prepared particles in the 0.5−2 μm size range that would be appropriate for RES imaging and could therefore replace the discontinued albumin colloids (Microlite). Our microspheres (Figure 1B and 2A) were made from the chelomer, or a blend of chelomer and a nonchelating commercial polymer, using a double emulsion, solvent extraction/evaporation procedure (*20*). In this water-in-oil-in-water (w/o/w) process, water-soluble or water-dispersible components are dissolved or dispersed in an aqueous solution, which is then emulsified in an organic solvent containing the chelomer. The primary water-in-oil emulsion (w/o) is then dispersed in a second aqueous phase, containing a suitable emulsifier, and forms a double emulsion (w/o/w). Solid microspheres are collected following the complete removal of the volatile organic solvent by

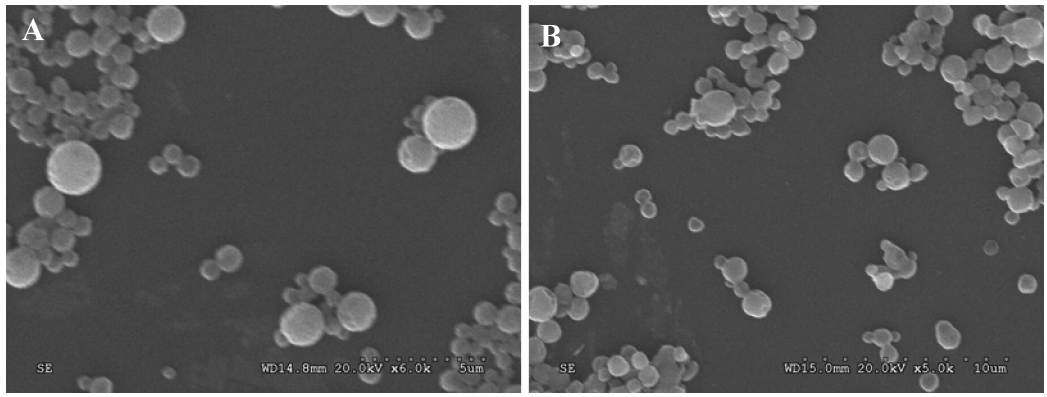

Figure 2. SEM pictures of the 10% blend PEGylated microspheres (A) before (scale bar 5 μm) and (B) after (scale bar 10 μm) radiolabeling.

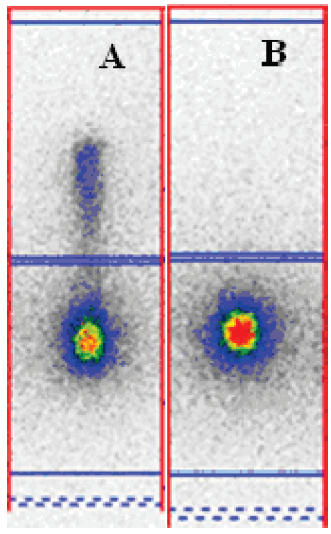

Figure 3. Developed TLCs of labeled microspheres made from (A) commercially available polymer (control) and (B) 100% chelomer. Saline was used as the mobile phase.

extraction into the surrounding water phase and evaporation. The first (inner) emulsion allows drug loading, and the second solidifies the particles. In the present studies, no drug was loaded into the microspheres. Instead, the microspheres consisted of a PLA core with the ligand bis(picolylamine) at the outer surface having the capability to bind metals. This technique of making microspheres does not involve chemical or physicochemical changes to the polymeric material; it is just a physical transformation of shape from a solid powder to microspheres.

Radiolabeling was readily achieved with the 100% chelomer microspheres. These microspheres suspended in the $[^{99m}Tc(H_2O)_3(CO)_3]^+$ solution and heated to 75 °C for 30 min took up 94.8 ± 1.5% of the radioactivity compared to 79.9 ± 7.4% for the control microspheres. The reaction conditions, especially heating at 75 °C, did not affect the physical appearance of the microspheres (Figure 2B). This is important for *in vivo* applications, as any changes in size and shape affect microsphere biodistribution (*21*).

Figure 3 compares the TLC of the chelomer-containing microspheres to that of control microspheres. Chelomer microsphere activity was found exclusively at $R_f = 0$, whereas an additional spot was observed for the control microspheres. The R_f of the additional spot was similar to that of $[^{99m}Tc(H_2O)_3(CO)_3]^+$, indicating random release. The labeling efficiency of the control polymer varied from sample to sample, as a result of nonspecific weak binding of $[^{99m}Tc(CO)_3]^+$ to the particles.

Once the initial radiochemical stability was confirmed, the labeling conditions were optimized in terms of chelomer fraction, heating time, and temperature. Table 2 shows the labeling efficiency for various blend compositions of microspheres reacted for varying times with $[^{99m}Tc(H_2O)_3(CO)_3]^+$. For all polymer blends containing more than 5% of the chelomer, the average labeling efficiency was about 95%, whereas the labeling efficiency for the 2% blend and the control (100% commercial PLA) were only slightly higher than 80%. Although low, the labeling efficiency for the 2% chelomer microspheres was consistent, while the results for the control (0% chelomer) varied wildly. This is depicted in Figure 4 by plotting the labeling efficiency of chelomer blends vs heating times for a subset of these experiments. Blended polymers containing 100% (A), 25% (B), or 10% (C) of the chelomer showed excellent labeling efficiency and high stability in the cysteine challenge. The control microspheres, 0% (D), however, were labeled less efficiently and could not withstand the cysteine challenge, as most of the radioactivity was released within 24 h.

For additional reaction times of 2, 5, and 120 min, only the 100% and 0% blends were examined. The 100% chelomer microspheres showed 86.8 ± 9.4%, 96.7 ± 0.5%, and 96.8 ± 3.1% radiolabeling efficiency, respectively, while the control microspheres took up only 62.3 ± 11.5%, 75.8 ± 11.8%, and 65.1 ± 6.1%. This indicates that a minimum reaction time of 5 min is needed to achieve labeling efficiencies suitable for clinical applications.

The thermodynamic stability of the radiolabeled complex for *in vivo* applications is generally evaluated by cysteine or histidine challenges, where the radioactive metal complex is placed in a concentrated solution of the competitive *in vivo* ligands cysteine or histidine (*22*). We performed a cysteine challenge after each labeling experiment. After 30 min of radiolabeling (Table 2), the cysteine challenge to microspheres consisting of 100% chelomer resulted in microsphere-bound activity of 89.3 ± 1.9% and 81.2 ± 2.2% at the 1 and 24 h time points, respectively. For the 0% chelomer microspheres (controls), only 37.9 ± 2.3% and 1.9 ± 3.6% of the activity remained microsphere-bound at the 1 and 24 h time points, respectively. This confirmed the stability of the complexation of $[^{99m}Tc(CO)_3]^+$ to the chelomer's bis(picolylamine) binding site after 24 h. Overall, for microspheres consisting of a more than 5% chelomer blend, stability after 15 to 60 min reaction time was approximately 95% activity as determined by the cysteine challenge. An average of 90% activity remained after 24 h of cysteine competition for the same groups.

To evaluate how much activity could be loaded onto the microspheres, the 5%, 10% and 25% chelomer blends were radiolabeled with increasing amounts of $[Tc(CO)_3]^+$ (74, 128, and 260 MBq). For all activities, the 10% blend chelomer had ≥93% labeling efficiency (Figure 5), with good cysteine

Table 2. Labeling Efficiency and Stability Results Measured at 37 °C for Microspheres Made from Polymer Blends with Different Amounts of Chelomer

		labeling efficiency (%)		cysteine challenge 1 h (%)		cysteine challenge 24 h (%)	
labeling time (min)	chelomer amount (%)	average	± S.D.	average	± S.D.	average	± S.D.
15	0	81.6	6.6	55.0	14.7	21.9	24.5
	2	82.9	1.6	62.2	0.2	42.5	0.4
	5	97.4	0.2	95.4	0.2	93.0	0.2
	10	96.6	1.4	93.5	2.5	89.7	3.4
	25	94.2	0.6	89.2	1.1	83.8	1.2
	100	94.3	0.5	89.1	0.3	81.0	0.3
30	0	80.0	7.4	53.4	17.1	44.5	25.2
	2	84.4	1.2	69.5	2.3	54.7	4.1
	5	96.5	0.2	94.3	0.2	91.7	0.1
	10	96.0	1.6	92.5	3.0	88.3	4.0
	25	93.9	0.3	88.6	0.6	82.3	0.9
	100	94.8	1.5	89.3	1.9	81.2	2.2
60	0	79.0	7.5	52.4	13.4	30.7	18.6
	2	88.1	0.9	78.1	0.7	67.2	1.2
	5	95.5	0.3	92.6	0.4	89.1	0.8
	10	94.6	1.3	90.4	2.6	85.4	3.7
	25	91.9	0.6	85.2	1.2	77.4	1.4
	100	92.0	0.6	84.7	1.0	74.9	1.4

Table 3. Organ/Blood Ratio of non-PEGylated and PEGylated ^{99m}Tc-Radiolabeled Microspheres and the ^{99m}Tc-Tricarbonyl Precursor at the 6 h Time Point ($n = 4$)

	Non-PEGylated ^{99m}Tc-microspheres		PEGylated ^{99m}Tc microspheres		$[^{99m}Tc(H_2O)_3(CO)_3]^+$	
organ	average	± S.D.	average	± S.D.	average	± S.D.
blood	1.00	0.00	1.00	0.00	1.00	0.00
heart	3.80	1.03	0.51	0.09	0.30	0.07
tumor	0.36	0.10	-	-	0.28	0.23
liver	17.10	1.00	29.47	3.99	1.06	0.16
kidneys	2.82	0.05	3.74	0.45	1.42	0.33
lungs	74.86	43.56	4.50	2.69	0.68	0.40
small intestine	0.75	0.10	0.59	0.05	0.34	0.04
brain	0.74	0.12	0.03	0.00	0.03	0.01
bladder	1.09	0.52	0.94	0.49	0.30	1.29
muscle	0.18	0.09	0.09	0.02	0.04	0.01
spleen	14.24	5.64	15.11	10.41	0.26	0.00
stomach	-	-	0.26	0.39	0.18	0.03

challenge results at 1 and 24 h. The 5% and 25% chelomer blends were only labeled with 74 and 128 MBq of activity and had 98% and 93% labeling efficiency, respectively.

We also evaluated the temperature of the radiolabeling reaction. As expected, lowering the radiolabeling temperature to less than 75 °C decreased thermal energy and led to increased reaction time or decreased labeling efficiency. For example, heating microspheres with 100% chelomer to 50 °C for 30 min resulted in a labeling efficiency of 50%. Since the biodegradable microspheres are sensitive to heat, we determined that 75 °C was the upper temperature limit to achieve labeling without affecting the polymer matrix integrity. Further shortening of the overall radiolabeling procedure would be possible only by speeding up the radiolabeling of the precursor $[Tc(H_2O)_3(CO)_3]^+$ using microwave heating (*23*).

The biodistribution of the 10% chelomer microspheres radiolabeled with 18.5 MBq of ^{99m}Tc (labeling efficiency 94%) (Figure 1E) was then investigated in mice after tail vein injection using microSPECT/CT imaging (Figure 6B) and organ activity analysis at the end of the experiment (Figure 7). Most microspheres accumulated in the liver, with additional substantial uptake in the lungs. The high lung uptake was unexpected since the microspheres sized between 1 and 2 μm (Figure 2A) were not large enough to clog the lung capillaries of between 5 and 7 μm. Two factors could be potential contributors to this uptake: the charge of the complex cation on the particle surface or *in vivo* agglomeration of the particles and accumulation in the lung capillaries. Upon checking, no *in vitro* aggregation of the radiolabeled microspheres was observed microscopically. No other organs received significant amounts of microspheres, and the tumors virtually excluded them.

As mentioned earlier, our experimental design did not include tumor-bearing mice initially, but since there were tumor-mice available destined to be sacrificed, we chose to use them for two main reasons. First, from literature data, it is well-known that microspheres are in general captured by the RES in the liver and spleen (*24*). Micrometer-sized particles are not expected to be taken up by a tumor—for that, they would have to be smaller than about 200 nm, which would increase their blood circulation time and make it possible for the particles to nonspecifically accumulate in newly grown tumors' leaky vasculature by the enhanced permeation and retention (EPR) effect (*25*). Using tumor-bearing animals would confirm this expectation. The second reason for using the available mice with tumors was that there is no published report about the biodistribution of the ^{99m}Tc-tricarbonyl precursor in the literature. Investigating this in mice with tumors might add more information to the reader than by doing it in normal mice. However, since there was no indication of tumor uptake with the microspheres, the later biodistribution study with the PEGylated microspheres was performed in mice without tumors.

To further investigate the significant lung uptake of the microspheres, we decided to make microspheres with additional PEGylated polymers incorporated into the surface (Figure 1C). PEGylation has been shown to enhance surface hydrophilicity of microspheres and to prevent agglomeration and clumping, not only *in vitro*, but also *in vivo* (*26*). To prepare PEGylated microspheres, 1.5% of a PEGylated polymer was simply added to the polymer blend during the preparation of the microspheres. The good labeling efficiency seen in non-PEGylated microspheres was maintained, as 2 mg of the PEGylated microspheres radiolabeled with 40 MBq of $[Tc(CO)_3]^+$ achieved a 97.8 ±

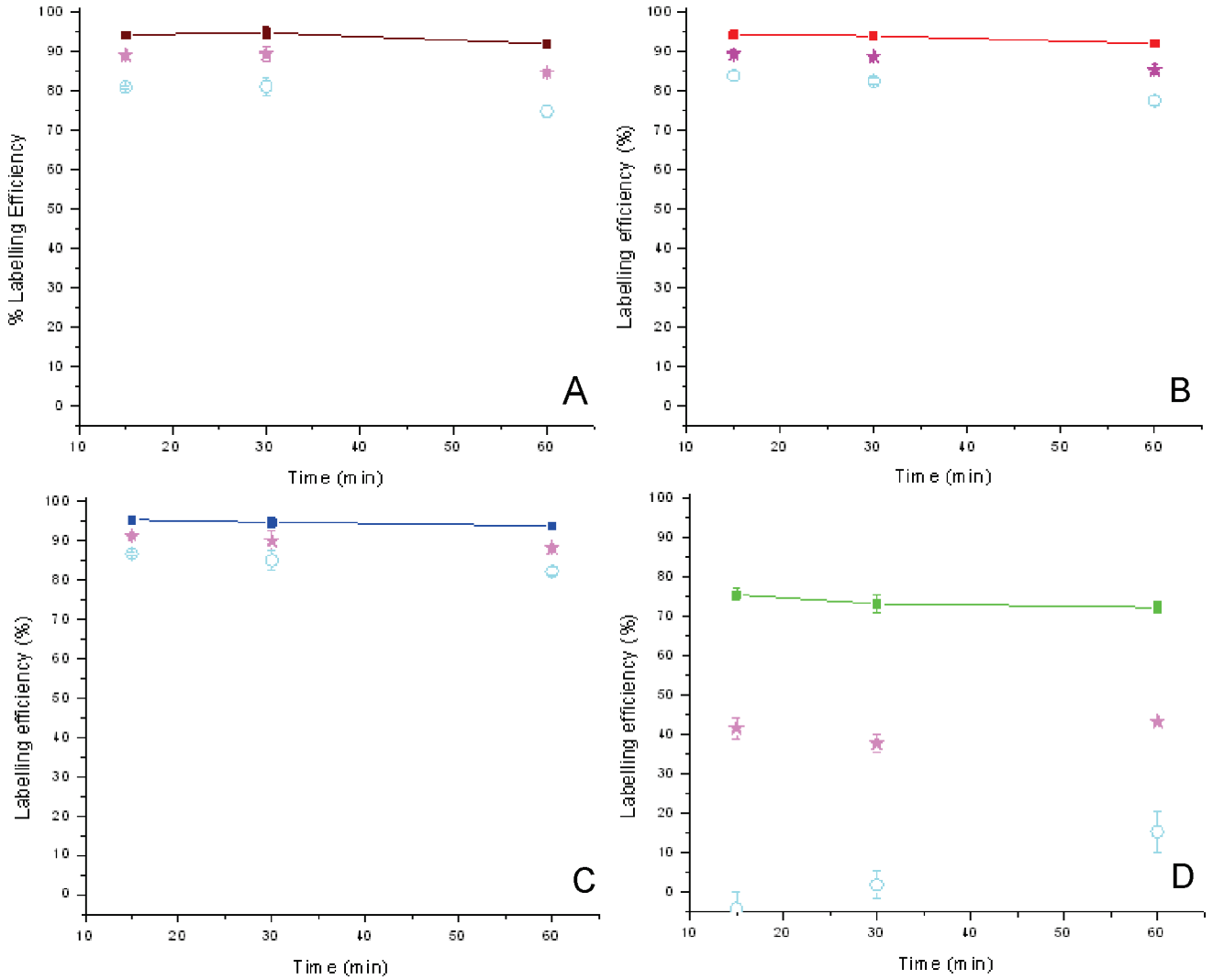

Figure 4. Plots of labeling efficiency vs initial reaction time along with the stability testing against cysteine for (A) 100%, (B) 25%, (C) 10%, and (D) 0%. Cysteine challenge results are given at 1 h (stars) and 24 h (hollow circles). For all experiments, 2 mg of microspheres were radiolabeled with 9.5 MBq (250 μCi) of $[Tc(CO)_3]^+$.

0.4% labeling efficiency. The radiochemical stability of these microspheres was as good as that of non-PEGylated microspheres: the cysteine challenge showed that 97% and 93% of the activity were still microsphere-bound after 1 and 24 h, respectively.

The biodistribution of PEGylated 10% chelomer microspheres radiolabeled with 18.5 MBq of ^{99m}Tc (Figure 1F) was also investigated in mice after tail vein injection. As seen by microSPECT/CT imaging (Figure 6C), almost all lung uptake could be avoided by using PEGylated microspheres. The charge on the microspheres was, therefore, not responsible for the lung uptake of microspheres observed previously. Uptake of the PEGylated microspheres by the liver increased, and all other organs received proportionally less of the radioactive microspheres (Figure 7).

To be able to evaluate the *in vivo* stability of the $[^{99m}Tc(CO)_3]^+$ complexation to the chelomer, an additional group of 4 animals received the same activity of the precursor complex $[^{99m}Tc(CO)_3(H_2O)_3]^+$ so that the biodistribution of the complex could be compared to that of the radiolabeled microspheres (Figure 6A). After 6 h, approximately one-third of the injected charged tricarbonyl compound was still found in the animals, mainly circulating in the blood. The heart with the highest blood concentration was, thus, highly visible in the SPECT scan. While a large part of the precursor complex $[^{99m}Tc(CO)_3(H_2O)_3]^+$ was

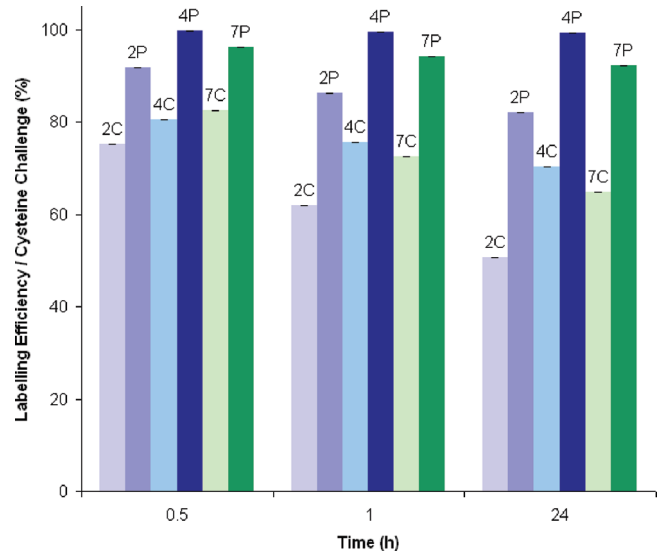

Figure 5. Graph showing labeling efficiency by increasing initial labeling activity from 74 MB (2 mCi) to 260 MBq (7 mCi) for 10% chelomer (P) vs control (C) microspheres. The first time point at 0.5 h is the labeling efficiency, while the 1 and 24 h time point are results of the cysteine challenge.

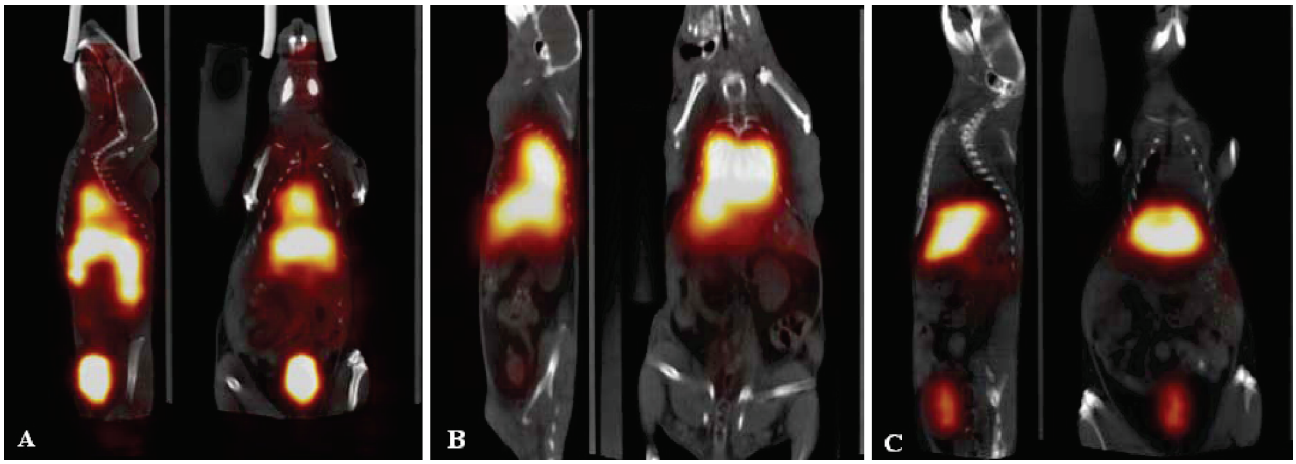

Figure 6. Sagittal (left) and coronal (right) microSPECT/CT images of (A) $[^{99m}Tc(H_2O)_3(CO)_3]^+$, (B) non-PEGylated microspheres, and (C) PEGylated microspheres 6 h after tail vein injection.

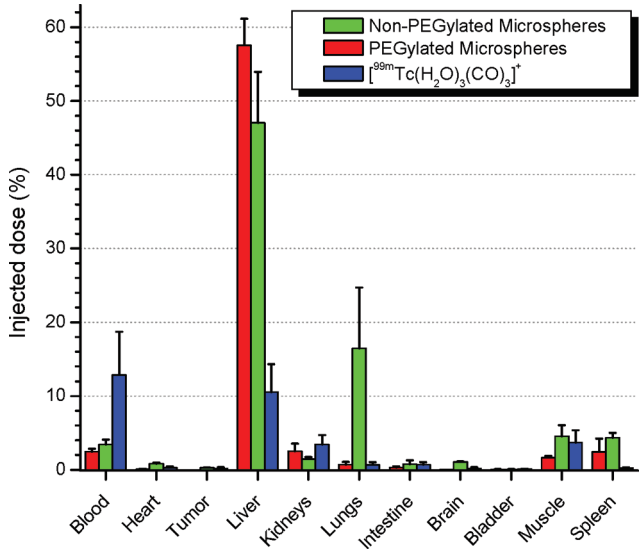

Figure 7. Biodistribution of non-PEGylated and PEGylated ^{99m}Tc-radiolabeled microspheres and the ^{99m}Tc-tricarbonyl precursor at the 6 h time point ($n = 4$).

excreted through the urine, some may have rapidly exchanged its three labile water molecules and ended up in coordination with potential donors from serum proteins, for example, transferrin, to coordinate the $[^{99m}Tc(CO)_3]^+$ core. Since transferrin is excreted and/or stored in the liver, the 11% of the activity found in the liver at the 6 h time point could further implicate transferrin as a carrier protein for $[^{99m}Tc(CO)_3]^+$.

The transferrin proteins are the most prominent metal binding proteins in the body fluids (*27*). Although it is the Fe^{3+} ion that is normally found in the active site of transferrin, this protein also has a high affinity for many other metal ions (*27, 28*). Transferrin's metal binding depends mainly on its structural organization. Both the C and the N lobes in the transferrins contain the same four donor atoms to bind various metal ions, two phenolic O from two tyrosines, an N from the histidine imidazole, and a carboxylate O from aspartic acid. It has been reported that accommodating metal ions depends on the conformation of both the apoprotein (metal-free protein) as well as the metal bound protein. Transferrin conformation changes from the initial open state to the closed state after metal binding. It is likely that the protein can accommodate $[^{99m}Tc(CO)_3]^+$ binding in the open state, since it acts as a potential tetra dentate ligand able to readily fill the three vacant positions around ^{99m}Tc. However, whether this binding puts much stress on the structure and hinders the conformational change (from open to closed), due to the size of $[^{99m}Tc(CO)_3]^+$, requires a thorough investigation. If transferrin's binding site cannot properly close, then the metal ion might be removed easily.

Biodistribution analysis at the 6 h time point via the organ/blood ratios (Table 3) confirmed that both PEGylated and non-PEGylated microspheres were mainly taken up by the monophagocytic system in the liver and spleen, and to a very similar extent. The only difference between the two types of microspheres was the 20-fold higher accumulation of the more hydrophobic, non-PEGylated microspheres in the lungs. While the reason for this lung accumulation is not known, the charge of the metal complex can be excluded as the cause, since both PEGylated and non-PEGylated microspheres had the same ligand moiety and generated similar complex cations. Agglomeration is more likely related to hydrophobic interactions with blood proteins, which can, for the most part, be prevented by PEGylation of the microspheres. Changes in the poly(ethylene glycol) chain length or in the total amount used (currently only 1.5%) might further reduce agglomeration in the lungs. The kidney to blood ratio of $[^{99m}Tc(CO)_3]^+$ after 6 h confirmed that the urinary system was its main path of excretion. The initially expected uptake of the positively charged $[Tc(CO)_3(H_2O)_3]^+$ in the heart, similar to that seen in the also positively charged radiopharmaceuticals sestamibi and tetrofosmin (*29*), was not confirmed (Table 3)—the $[^{99m}Tc(CO)_3(H_2O)_3]^+$ compound is likely not sufficiently lipophilic. The low heart to blood ratio of 0.30 suggests that the highly visible heart during SPECT imaging at the 6 h time point was due to the large volume of radioactive blood in the heart and not due to local binding of the radioactive compound to the myocardium.

Unfortunately, colloidal albumin kits in the same size range as our particles are no longer available, making direct comparison of our labeling and biodistribution results difficult. We have, however, compared our findings to those by Scheffel et al., who described the preparation of human serum albumin (HSA) microspheres with an average size of 0.6 μm (*24*). The values for the percentage of injected dose per organ measured after 4.25 h were similar to our findings measured after 6 h (Figure 7). For example, the blood activity was 0.9% vs 2.5%; the liver uptake was 73.2% vs 57.6%; the spleen uptake was 1.0% vs 2.5%, and finally the lung uptake was 0.3% vs 0.7%, accordingly (Scheffel et al. vs our data for the PEGylated microspheres). Differences might have mainly to do with the different size distribution and/or time point of analysis.

In conclusion, chelomer-formulated microspheres are promising candidates for imaging, as they exhibit excellent radiolabeling efficiency and radiochemical stability. The PEGylated microspheres showed no agglomeration, a key factor for *in vivo* utilization of these particles. Therefore, the PEGylated chelomer microspheres are excellent tools for RES imaging. Other potential applications with the same microspheres of larger size (around 10 μm) include lung perfusion imaging. And even larger, around 40 μm, the biodegradable microspheres could be radiolabeled with the β-emitter ^{188}Re and used for the therapeutic radioembolization of liver tumors. The easy and complete kit-based labeling and the fact that the particles do not agglomerate will allow for reliable and repeatable imaging, and potentially even therapy. Furthermore, all biohazards connected with the handling of blood products are eliminated with these nontoxic, biocompatible, and biodegradable microspheres.

ACKNOWLEDGMENT

We thank Dr. Troy Farncombe, Chantal Saab, and Rod Rhem at McMaster's Centre for Preclinical and Translational Imaging in Hamilton, Ontario, Canada, for excellent imaging support. We also thank Scott McNaughton, radiopharmacist at McMaster's University Health Centre, for providing ^{99m}Tc and space for the radiolabeling, and Dr. Don Lyster, at Vancouver General Hospital, Vancouver, British Columbia, Canada for many discussions. We appreciate support for this research from a Natural Sciences and Engineering Research Council of Canada (NSERC) grant.

LITERATURE CITED

(1) Saha, G. B. (2004) *Fundamentals of nuclear pharmacy*, 5th ed., Springer, New York.

(2) Rhodes, B. A., Zolle, I., Buchanan, J. W., and Wagner, H. N. (1969) Radioactive albumin microspheres for studies of the pulmonary circulation. *Radiology 92*, 1453–1460.

(3) Davis, M. A. (1975) Particulate radiopharmaceuticals for pulmonary studies, in *Radiopharmaceuticals* (Subramaniam, B., Rhodes, B., Cooper, D. R., Sodd, V. J., Eds.) pp 267−281, Society of Nuclear Medicine, Reston, VA.

(4) Sty, J. R., and Conway, J. J. (1985) The spleen: development and functional evaluation. *Semin. Nucl. Med. 15*, 276–298.

(5) Desai, A. G., and Thakur, M. L. (1985) Radiopharmaceuticals for spleen and bone marrow studies. *Semin. Nucl. Med. 15*, 229–38.

(6) Toki, H., Hersh, E. M., Murphy, S., Glenn, H., Haynie, T. P., and White, R. A. (1981) Use of mini-microaggregated albumin to study reticuloendothelial system (RES) function in *C. parvum*-treated animals. *Int. J. Immunopharmacol. 3*, 147–52.

(7) Bolognesi, M., Merkel, C., and Gatta, A. (1987) The use of human albumin microspheres tagged with ^{99m}Tc in the evaluation of the removal capacity of the reticuloendothelial system. *Eur. J. Nucl. Med. 13*, 254–257.

(8) Mirzaei, S., Knoll, P., Hoffmann, B., Kreuzer, W., and Kohn, H. (2001) Optimized mammary lymphoscintigraphy using larger colloid particles. *J. Nucl. Med. 42*, 826.

(9) Fowler, J. C., Solanki, C. K., Barber, R. W., Ballinger, J. R., and Peters, A. M. (2007) Dual-isotope lymphoscintigraphy using albumin nanocolloid differentially labeled with ^{111}In and ^{99m}Tc. *Acta Oncol. 46*, 105–110.

(10) Zhao, H., Saatchi, K., and Häfeli, U. O. (2009) Preparation of biodegradable magnetic microspheres with poly(lactic acid) coated magnetite. *J. Magn. Magn. Mater. 321*, 1356–1363.

(11) Schneider, T., Zhao, H., Jackson, J. K., Chapman, G. H., Dykes, J., and Häfeli, U. O. (2008) Use of hydrodynamic flow focusing for the generation of biodegradable camptothecin-loaded polymer microspheres. *J. Pharm. Sci. 97*, 4943–4954.

(12) Saatchi, K., and Häfeli, U. O. (2007) One-pot syntheses, coordination and characterization of application-specific biodegradable ligand-polymers. *Dalton Trans. 39*, 4439–4445.

(13) Zastre, J., Jackson, J., Bajwa, M., Liggins, R., Iqbal, F., and Burt, H. (2002) Enhanced cellular accumulation of a P-glycoprotein substrate, rhodamine-123, by Caco-2 cells using low molecular weight methoxypolyethylene glycol-block-polycaprolactone diblock copolymers. *Eur. J. Pharm. Biopharm. 54*, 299–309.

(14) Egli, A., Alberto, R., Tannahill, L., et al. (1999) Organometallic Tc-99m-aquaion labels peptide to an unprecedented high specific activity. *J. Nucl. Med. 40*, 1913–1917.

(15) Alberto, R., Ortner, K., Wheatley, N., Schibli, R., and Schubiger, P. A. (2001) Synthesis and properties of boranocarbonate: a convenient in situ CO source for the aqueous preparation of $[^{99m}Tc(OH_2)_3(CO)_3]^+$. *J. Am. Chem. Soc. 123*, 3135–3136.

(16) Amann, A., Decristoforo, C., Ott, I., et al. (2001) Surfactant protein B labeled with $[Tc\text{-}99m(CO)_3(H_2O)_3]^+$ retains biological activity in vitro. *Nucl. Med. Biol. 28*, 243–250.

(17) Petrig, J., Schibli, R., Dumas, C., Alberto, R., and Schubiger, P. A. (2001) Derivatization of glucose and 2-deoxyglucose for transition metal complexation: substitution reactions with organometallic 99mTc and Re precursors and fundamental NMR investigations. *Chemistry 7*, 1868–73.

(18) Waibel, R., Treichler, H., Schaefer, N. G., et al. (2008) New derivatives of vitamin B12 show preferential targeting of tumors. *Cancer Res. 68*, 2904–11.

(19) Zhao, H., Gagnon, J., Häfeli, U. O. (2007) Process and formulation variables in the preparation of injectable and biodegradable magnetic microspheres. *Biomagn. Res. Technol. 5:2*.

(20) Cleland, J. L. (1998) Solvent evaporation processes for the production of controlled release biodegradable microsphere formulations for therapeutics and vaccines. *Biotechnol. Prog. 14*, 102–107.

(21) Arshady, R., Monshipouri, M. (2001) Targeted delivery of microparticulate carriers: particle size controlled targeting, in *Microspheres, Microcapsules & Liposomes: Medical & Biotechnology Applications*, (Arshady, R., Ed.) pp 410−414, Vol MML2, Kentus, London.

(22) Hnatowich, D. J., Virzi, F., Fogarasi, M., Rusckowski, M., and Winnard, P. (1994) Can a cysteine challenge assay predict the in vivo behavior of ^{99m}Tc-labeled antibodies? *Nucl. Med. Biol. 21*, 1035–44.

(23) Causey, P. W., Besanger, T. R., Schaffer, P., and Valliant, J. F. (2008) Expedient multi-step synthesis of organometallic complexes of Tc and Re in high effective specific activity. A new platform for the production of molecular imaging and therapy agents. *Inorg. Chem. 47*, 8213–21.

(24) Scheffel, U., Rhodes, B. A., Natarajan, T. K., and Wagner, H. N. (1972) Albumin microspheres for study of the reticuloendothelial system. *J. Nucl. Med. 13*, 498–503.

(25) Tanaka, T., Shiramoto, S., Miyashita, M., Fujishima, Y., and Kaneo, Y. (2004) Tumor targeting based on the effect of enhanced permeability and retention (EPR) and the mechanism of receptor-mediated endocytosis (RME). *Int. J. Pharm. 277*, 39–61.

(26) Wattendorf, U., and Merkle, H. P. (2008) PEGylation as a tool for the biomedical engineering of surface modified microparticles. *J. Pharm. Sci. 97*, 4655–69.

(27) Baker, H. M., Baker, C. J., Smith, C. A., and Baker, E. N. (2000) Metal substitution in transferrins: specific binding of cerium(IV) revealed by the crystal structure of cerium-substituted human lactoferrin. *J. Biol. Inorg. Chem. 5*, 692–8.

(28) Sun, H., Li, H., and Sadler, P. J. (1999) Transferrin as a metal ion mediator. *Chem. Rev. 99*, 2817–42.

(29) Schaefer, W. M., Moka, D., Brockmann, H. A., Schomaecker, K., and Schicha, H. (2002) ^{201}Tl, ^{99m}Tc-MIBI, ^{99m}Tc-tetrofosmin and ^{99m}Tc-furifosmin: relative retention and clearance kinetics in retrogradely perfused guinea pig hearts. *Nucl. Med. Biol. 29*, 243–54.

(30) Tsopelas, C. (2001) Particle size analysis of ^{99m}Tc-labeled and unlabeled antimony trisulfide and rhenium sulfide colloids intended for lymphoscintigraphic application. *J. Nucl. Med. 42*, 460–466.

(31) Harbert, J. C. (1996) Radiocolloid therapy of cystic brain tumors, in *Nuclear medicine: Diagnosis and therapy* (Harbert, J. C., Eckelman, W. C., and Neumann, R. D., Eds.) pp 1083−1091, Thieme Medical Publishers, New York.

(32) Nolan, T. R., Grady, E. D., Crumbley, A. J., Larose, J. H., and Cheek, W. V. (1975) Internal hepatic radiotherapy: I. Organ distribution of colloid Cr-(P-32)PO4 injected into a peripheral vein, the portal vein, or the arterial supply of the gastrointestinal tract in the rat. *Am. J. Roentg. Rad. Ther. Nucl. Med. 124*, 590–595.

(33) Anghileri, L. J. (1968) Studies on colloidal chromic phosphate: an improved method of preparation and in situ precipitation by injection of papain. *Int. J. Appl. Radiat. Isot. 19*, 415–20.

(34) Salem, R., and Hunter, R. D. (2006) Yttrium-90 microspheres for the treatment of hepatocellular carcinoma: a review. *Int. J. Radiat. Oncol. Biol. Phys. 66*, S83−S88.

(35) Kennedy, A., Nag, S., Salem, R., et al. (2007) Recommendations for radioembolization of hepatic malignancies using yttrium-90 microsphere brachytherapy: a consensus panel report from the radioembolization brachytherapy oncology consortium. *Int. J. Radiat. Oncol. Biol. Phys. 68*, 13–23.

BC900066J